Analysis of Extended Threshold Wavelength Photoresponse in Non-symmetrical p-GaAs/AlGaAs Heterostructure Photodetectors

D. Somvanshi, D. Chauhan, Y.-F. Lao, A. G. Unil Perera, *Fellow, IEEE,* L. H. Li, S. P. Khanna and E. H. Linfield

***Abstract*—We analyze the extended threshold wavelength photoresponse beyond the standard threshold limit ($\lambda_t = 1.24/\Delta$, where Δ is the activation energy) in non-symmetrical p-GaAs/AlGaAs heterostructure photodetectors with a barrier energy offset. We propose that hot-cold hole carrier interactions in the p-GaAs absorber are responsible for the threshold wavelength extension. Experimental results are analyzed by considering a quasi-Fermi distribution of hot holes at a hot hole temperature (T_H), which is much higher than the lattice temperature (T_L). The experimental photoresponse is fitted using an escape cone model, modified with a quasi-Fermi level (E_{quasiF}). The simulated results are found to be in good agreement with experimental data, justifying the model used.**

***Index Terms*—quasi-Fermi distribution, threshold wavelength, photoresponse, heterostructures, temperature.**

I. INTRODUCTION

Hot-carrier effects in semiconductor heterostructures have played a major role in the development of photodetectors [1-3]. They are governed principally by carrier-carrier and carrier-phonon scattering processes, which are also of fundamental interest for the study of semiconductor physics [4-6]. The dynamics of hot carriers in bulk GaAs [4-6], and in GaAs/AlGaAs quantum wells (QWs) [7-9] and heterostructures [5, 10], have been widely studied by hot carrier spectroscopy. In general, hot carriers are created in energy states above the band edge, interact with the lattice vibrations and cold carriers through carrier-carrier interactions; this leads to a quasi-equilibrium distribution at a carrier temperature that is much higher than the lattice temperature [4, 5]. The relaxation processes of hot carriers in bulk GaAs, GaAs/AlGaAs QWs structure, and heterostructures have been studied extensively by optical spectroscopy with ultrashort laser pulses [9, 11]. In most experiments on femtosecond [9, 12] and picosecond [13] time scales, a hot electron-hole plasma is created by interband excitation and the relaxation behavior of carriers is then monitored through the time evolution of the absorption or luminescence. Such time-resolved optical experiments, using pico- and femtosecond laser pulses, allow the creation of well-defined non-equilibrium conditions, and provide direct information on the microscopic scattering processes by which the carriers relax into quasi-equilibrium [7, 9, 13].

Recently, a new concept of very long-wavelength infrared (VLWIR) photodetection was proposed by Lao *et al.* [14] based on hot hole effects, which enable a spectral extension of the photoresponse beyond the standard limit set by the 'spectral rule' $\lambda_t = 1.24/\Delta$, where Δ is the activation energy. Typically, λ_t and Δ is a good measure of performance in a variety of detectors, including GaAs/AlGaAs QWs [7-9] and heterostructures [5, 10]. However, there was no clear agreement between the observed extended wavelength photoresponse and the designed λ_t in non-symmetrical p-GaAs/AlGaAs heterostructures [14-16]. Therefore, a precise analysis is needed to understand fully the wavelength extended photoresponse; further optimize the performance; and, control the threshold of the extended wavelength photoresponse. This mechanism could then also be used to design IR photodetectors in other materials system and optimize detectors for specified threshold wavelengths.

Although various models have been reported to explain the spectral photoresponse of a variety of heterojunction detectors [17-20], none of those are able to explain the origin of the extended threshold wavelength photoresponse in non-symmetrical GaAs/AlGaAs heterojunction photodetectors. Nevertheless, it was believed that the dynamics of the hot-cold hole interaction played a crucial role [14]. In this paper, we present a theoretical explanation of the experimentally observed extended threshold wavelength photoresponse, by modelling the quasi-Fermi distribution of hot holes in the absorber. This follows the interpretation of hot carrier

This work was supported, in part, by the U.S. Army Research Office under Grant No. W911 NF-15-1-0018 and, in part, by National Science Foundation (NSF) under Grant No. ECCS-1232184. Funding was also received from the European Community's Seventh Framework Programme (FP7) under Grant Agreement No. 247375 "TOSCA".

D. Somvanshi, D. Chauhan and A. G. U. Perera are at the Department of Physics and Astronomy, Georgia State University, Atlanta, 30303 GA (e-mail: uperera@gsu.edu)

Y. F. Lao was at Georgia State University, Atlanta, 30303, USA. He is now working as a laser device engineer at Archcom Technology Inc., South Plainfield, NJ.

S. P. Khanna was at the School of Electronic and Electrical Engineering, University of Leeds, Leeds LS2 9JT, UK; He is now at the National Physical Laboratory, India.

L. H. Li and E. H. Linfield are at the School of Electronic and Electrical Engineering, University of Leeds, Leeds LS2 9JT, UK

spectroscopy in GaAs/AlGaAs heterostructures by Shah [5, 6] which describes the formation of hot carrier distribution under high intensity photoexcitation. The work reported by Ulbrich [21] also outlines the basic mechanisms resulting from photoexcitation of electron-hole pairs in semiconductors, but under conditions of low excitation intensity and low temperature .

II. ANALYSIS OF EXTENDED THRESHOLD WAVELENGTH PHOTORESPONSE

Schematic valence band (VB) diagrams of non-symmetrical and symmetrical p-type GaAs/$Al_xGa_{1-x}As$ heterostructures are illustrated in figs. 1(a)-(d), and are used to explain the possible mechanism for an extended threshold wavelength photoresponse. The structures consist of three p-type GaAs regions (doped at $p = 1\times10^{19}$ cm^{-3}, based on our previous work Ref. [17], Matsik et al. (2009)): the injector, absorber and collector. By varying the Al fractions in the undoped $Al_xGa_{1-x}As$ barriers, an energy offset between the barriers above and below the absorber can be created (figs 1(a)-(c)), in contrast to the situation for symmetrical heterostructures (fig 1(d)). In our analysis, we assume that the non-symmetrical and symmetrical heterostructures are both excited by a broad, black body source with peak intensity 2.8 mW/cm^2 to measure the photoresponse spectra (Perkin–Elmer system 2000 Fourier transform infrared (FTIR) spectrometer), the optical power spectrum of which was reported in [14].

In fig.1(a), Δ_{max} is the maximum barrier height (BH) at the injector/absorber junction, $\boldsymbol{\delta}E_v$ is the barrier energy offset, Δ_C is the BH at the absorber/collector junction, and E_F is the Fermi level at the lattice temperature (T_L). In Fig. 1(b), the blue wavy arrow represents an incident photon with an energy exceeding injector barrier, whilst the red wavy arrow in the absorber shows an incident photon with an energy below Δ_{max}, and represents the long wavelength absorption. The dotted blue arrow inside the absorber shows the movement of hot holes, the solid (red) dots, and an empty (green) dot represent hot holes and cold holes in the absorber, and E_{quasiF} represents the quasi-Fermi level at hot hole temperature (T_H).

Upon incidence of light from an external optical source, hot holes are created in the injector, absorber and collector regions for both symmetrical and non-symmetrical heterostructures. However, only hot carriers arising from the injector are considered in non-symmetrical heterostructures since the collector contribution is negligible owing to energy relaxation in the thick collector barrier. Hot holes with energy $>\Delta_{max}$ will surmount the injector barrier, and interact with cold holes in the absorber. In non-symmetrical heterostructure, a net flow of hot holes will then observed into the collector, owing to the difference in barrier heights, ΔE_v. The dynamics of hot-cold holes in the p-GaAs absorber can be explained based on hot carrier effects [5]. Upon interaction, exchange of energy takes place through hole-hole and hole-phonon scattering that leads to the formation of a quasi-Fermi distribution (E_{quasiF}) in the absorber at a hot hole temperature (T_H) which is significantly greater than the lattice temperature (T_L). In figs.1(b) and (c), the solid dual arrow connecting hot holes and cold holes represent interaction and exchange of energy. The distribution of hot holes at this quasi-Fermi level will lead to escape of hot holes across the collector barrier when a long wavelength photon is absorbed (red wavy arrow) the ‘so-called’ extended threshold wavelength photoresponse; the absorbed photon would have insufficient energy to cause excitation over the injector barrier by itself.

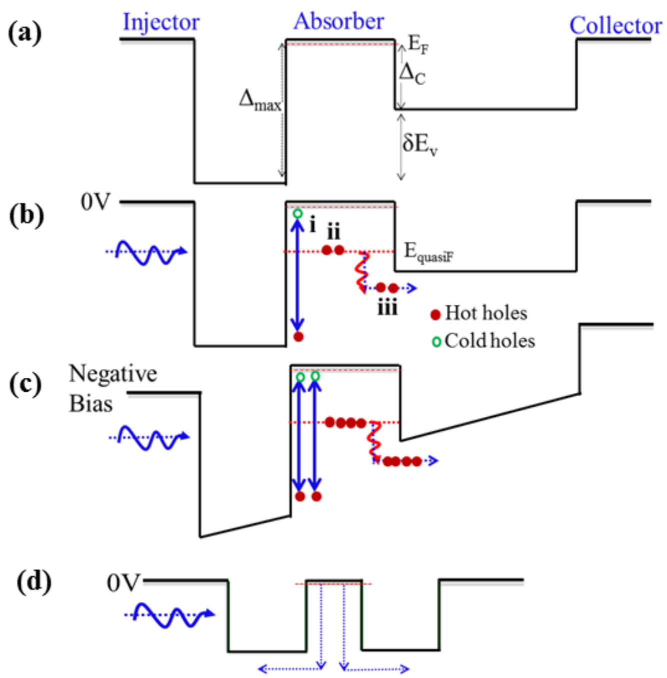

Fig.1 (a) Schematic VB diagram of a non-symmetrical heterostructure, where Δ_{max} is the maximum barrier height (BH) at the injector/absorber junction, $\boldsymbol{\delta}E_v$ is the barrier energy offset, Δ_C is the BH at the absorber/collector junction and E_F is the Fermi level at the lattice temperature (T_L) (b) Upon application of light (blue wavy arrow) incident from a broad black body optical source, hot holes with energies > Δ_{max} will be excited over the injector barrier, with a contribution also arising from absorption of incident radiation in the absorber and collector regions. We have divided the hot-cold hole dynamics in the p-GaAs absorber into three sequential process: (i) Exchange of energy (shown by solid dual arrows between the hot and cold holes) through interaction of hot holes and cold holes in the absorber; (ii) Formation of quasi-Fermi level E_{quasiF} at a hot hole temperature $T_H >> T_L$ and, (iii) Escape of hot holes from the quasi-Fermi level across the absorber/collector junction, upon incident of a long wavelength photon (red wavy arrow) (c) Upon application of negative bias, the hot holes passing from the injector to absorber have a greater energy, which increases the number of hot holes in the absorber. It is thus expected that the degree of extended photoresponse would increases with bias. (d) With the incident light from the same broad black body optical source in symmetrical heterostructure, hot holes which have sufficient energy to surmount the injector and collector barriers, can pass between the injector, collector, and absorber. However, there is no net flow of hot holes owing to the symmetry.

The schematic VB diagram of the non-symmetrical heterostructure under application of negative bias is shown in fig.1(c). Upon application of a negative bias, the energy of holes passing over the injector barrier increases, leading to a greater transfer of energy to the cold holes in the absorber and this increases the number of hot holes in the absorber. Hence the number of hot holes escaping from the quasi-Fermi distribution over the collector barrier also increases, thereby increasing the strength of the extended photoresponse.

The schematic VB diagram of a symmetric heterostructure is shown in Fig. 1(d) at zero bias. Upon application of incident light from the same optical source, hot holes will surmount the injector barrier, with contributions also arising from the absorber and collector. Furthermore, hot holes will interact with cold holes and exchange their energy, and a quasi-Fermi distribution will be formed in the absorber. However, current will flow equally across the injector and absorber barriers, from the quasi-Fermi level, and there will be no net flow of hot holes observed. Therefore, upon application of bias, photoresponse with conventional threshold wavelength will be observed in symmetric heterostructure.

The possible escape pathways of hot holes are from the heavy-hole (HH), light-hole (LH) and split-off (SO) bands to the quasi-Fermi level across the collector barrier. In the first mechanism, light absorption, from a long wavelength photon, leads to the transition of hot holes from the HH and LH band to the SO bands which is followed by internal photoemission, and escape over the collector barrier [17]. In the second mechanism, a portion of the hot holes lose some of their energy via different scattering mechanism and relax to the band edge of the LH or HH bands and then escape over the collector barrier [17]. The escape probability can be determined by using an escape cone model [22].

III. THEORETICAL SIMULATION USING ESCAPE CONE MODEL

To validate that the quasi-Fermi distribution (E_{quasiF}) of hot holes in the p-GaAs absorber is responsible for the extended wavelength photoresponse, we have used an escape-cone model [22] to simulate the extended photoresponse spectrum. In this model, free-carrier absorption, described by Drude theory, is considered as the primary optical absorbing mechanism [19]. The responsivity of the heterostructure detector depends on the total quantum efficiency (η) and is given by the following relation [17-19]

$$R = q\eta\lambda / hc \tag{1}$$

where q is the electron charge, c is the speed of light and h is the Planck's constant. The total quantum efficiency (η) is the product of the photon absorption probability (η_a), the internal quantum efficiency (η_i), and the hot carrier transport probability (η_t), and is given by:

$$\eta = \eta_a \eta_i \eta_t \tag{2}$$

The value of η_a and η_t were calculated using the model described in [18, 19]. η_i was calculated using an escape cone model [22], and is defined as the ratio of the number of carriers at the excited E_{quasiF} that have sufficient kinetic energy to overcome the barrier, associated with the momentum component normal to the interface, to the total number of excited carriers. Calculation of η_i can take into account scattering with cold holes and phonons, as given by[22]:

$$\eta_i = \eta_0 + \left[1 - \frac{\eta_0}{\eta_M}\right]\gamma\eta_1 + \left[1 - \frac{\eta_0}{\eta_M}\right]\cdot\left[1 - \frac{\eta_1}{\eta_M}\right]\gamma^2\eta_1 + \ldots \tag{3}$$

where $\eta_n = \eta_0(E - nh\nu)$ and $\gamma = L_h / (L_e + L_h)$

Here, n is the number of scattering events, η_M is the maximum quantum efficiency, and the value of η_0 is defined as the fraction of hot holes captured prior to any bulk scattering events, and is given by,

$$\eta_0 = \frac{L^*}{W}\cdot\left(1 - e^{-W/L^*}\right)^{1/2}\cdot\eta_{Ideal} \tag{4}$$

where W is the width of absorber, and η_{Ideal} is the ideal quantum efficiency, $L^* = L_h \times L_p / (L_h + L_p)$ is the reduced scattering length for hot hole-cold holes, L_h is the hole-hole scattering length for hot-cold holes and L_p represents elastic scattering of hot holes with phonons and impurities, and multiple reflections of the excited hot holes from the surfaces of the absorber [22]. In this simulation, we have only modified the escape cone model by changing the Fermi distribution at E_F to the perturbed E_{quasiF}.

IV. COMPARISON WITH EXPERIMENTS

The simulated photoresponse obtained from the escape-cone model with a modified hot-hole Fermi distribution, leading to a modified effective Δ, were compared with experimentally measured results. The spectral photoresponse of three heterostructure photodetectors with symmetrical (LH1002) and non-symmetrical (SP1001, SP1007) configurations were measured at 5.3 K; fabrication and characterization have already been reported elsewhere [14, 23, 24]. The valence band (VB) diagram of sample LH1002 with a p-type doped GaAs absorber sandwiched between two flat (60 nm) $Al_{.57}Ga0_{.43}As$ barriers is shown in fig 2(a). Fig. 2(b) and 2(c) show VB diagrams of SP1001 (flat injector barrier with **δ**E_v = 0.10 eV) and SP1007 (graded injector barrier with Al fraction varying from 0.45 to 0.75 and **δ**E_v = 0.10 eV), respectively. The activation energy (Δ) is defined as the energy difference between the Fermi level in the p-type GaAs and the valence band-edge of the $Al_xGa_{1-x}As$ barrier. For Al mole fraction values (x) of 0.45, 0.57 and 0.75, Δ is calculated to be 0.25 eV, 0.32 eV and 0.42 eV, respectively. Details of Δ and **δ**E_v for all the samples, calculated by taking into account band offsets at the heterointerface and doping-induced bandgap narrowing [14], are compared in Table.1. Spectral responses were measured using a Perkin–Elmer system 2000 Fourier transform infrared (FTIR) spectrometer. A bolometer with known sensitivity was used for background measurements and calibrating the responsivity. In general, holes in the p-GaAs absorber interact with incident photons and, when they gain sufficient energy to surmount the barrier, travel in both directions, i.e. towards the bottom (BC) and top (TC) contacts, giving rising to forward and reverse photocurrents. As a consequence, the net photocurrents are determined by the balance of the photoemission efficiencies associated with movement of holes in the forward and reverse directions [23].

TABLE.1: COMPARISON OF THE VALUES OF ACTIVATION ENERGY AND ENERGY OFFSET FOR LISTED DEVICES. IN ALL SAMPLES THE GaAs ABSORBER HAS A DOPING DENSITY OF p = 1×10^{19} cm^{-3}.

Samples	Activation Energy (eV)			Barrier Energy offset δE_v (eV)
	Δ_{max}	Δ_{min}	Δ_c	
LH1002	0.32	0.32	0.32	0
SP1001	0.42	0.42	0.32	0.10
SP1007	0.42	0.25	0.32	0.10

Under zero applied bias, in LH1002 ($\boldsymbol{\delta}E_v = 0$) the net flow of photoexcited holes in both direction is the same. However, for SP1001 and SP1007, because $\boldsymbol{\delta}E_v = 0.10$ eV, the net photoemission efficiency is not equal owing to the difference between the heights of the barriers below and above the absorber. Therefore, there exists a net flow of current from absorber to the collector, even at zero bias. The spectral photoresponse of LH1002 at 5.3 K for different biases, ranging from 0 to -0.5 V is shown in fig. 2(d). The threshold energy of spectral photoresponse is determined by temperature-dependent internal photoemission spectroscopy (TDIPS) fitting, where the quantum yield defined as the number of collected hot holes per incident photon and is proportional to the multiplication of the spectral responsivity with photon energy[25]. The quantum yield is plotted as a function of photon energy in the inset of fig. 2(d), and used to calculate the threshold energy of the photoresponse. The details of the TDIPS principle and the formalism for interpreting yield spectra by a fitting procedure are described in Ref.[25]. The threshold energies calculated from TDIPS fitting are consistent with the designed wavelength photoresponse when the bias is between 0 to -0.5 V [24]. The small increase in the TDIPS threshold wavelength with bias is a result of the image force lowering effect [24] present in heterostructures.

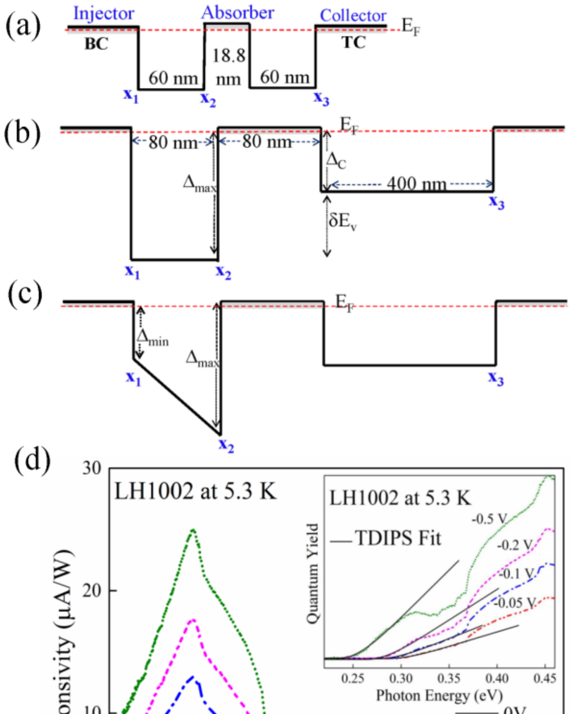

Fig. 2 (a) The VB diagram of sample LH1002, which has a symmetric band configuration ($\boldsymbol{\delta}E_v = 0$) and consists of two AlGaAs flat barriers with equal thickness and equal mole fraction, i.e. $x_1 = x_2 = x_3 = 0.57$. (b) Non-symmetrical VB structure of sample SP1001, where $x_1 = 0.75$, $x_2 = 0.75$ and $x_3 = 0.57$, and $\boldsymbol{\delta}E_v = 0.10$ eV is the energy offset between the barriers below and above the absorber; $\Delta_{max} = 0.42$ eV and $\Delta_C = 0.32$ eV (c) Non-symmetrical graded barrier structure of sample SP1007 which has a similar device structure to SP1001 except that $x_1 = 0.75$, $x_2 = 0.45$ and $x_3 = 0.57$; $\boldsymbol{\delta}E_v = 0.10$ eV, with $\Delta_{max} = 0.42$ eV and $\Delta_{min} = 0.25$ eV (d) Spectral response of LH1002 at 5.3 K, for different bias voltages, ranging from 0 to -0.5 V. The inset shows TDIPS fitting of the experimental data to determine the threshold energy; the observed spectral response matches the designed threshold wavelength.

Fig. 3 (a) shows the spectral response of sample SP1001 at 5.3 K for the voltages ranging from 0 V to -0.5 V. An extended threshold wavelength response up to ~ 36 μm is observed between -0.3 V and -0.5 V, together with the conventional response. Further, increasing bias voltage > -0.6 V, intensity of extended photoresponse started decreasing and at higher than > -1.2 V, extended threshold photoresponse became zero and photoresponse with conventional threshold wavelength is observed. The inset of fig. 3(a) shows the weak extended photoresponse of SP1001 at zero bias. We can interpret this as, due to barrier energy offset in the heterostructure, an extended photoresponse is seen at 0V in SP1001, whereas no extension was observed in the symmetric barrier structure as shown in fig. 2(d).

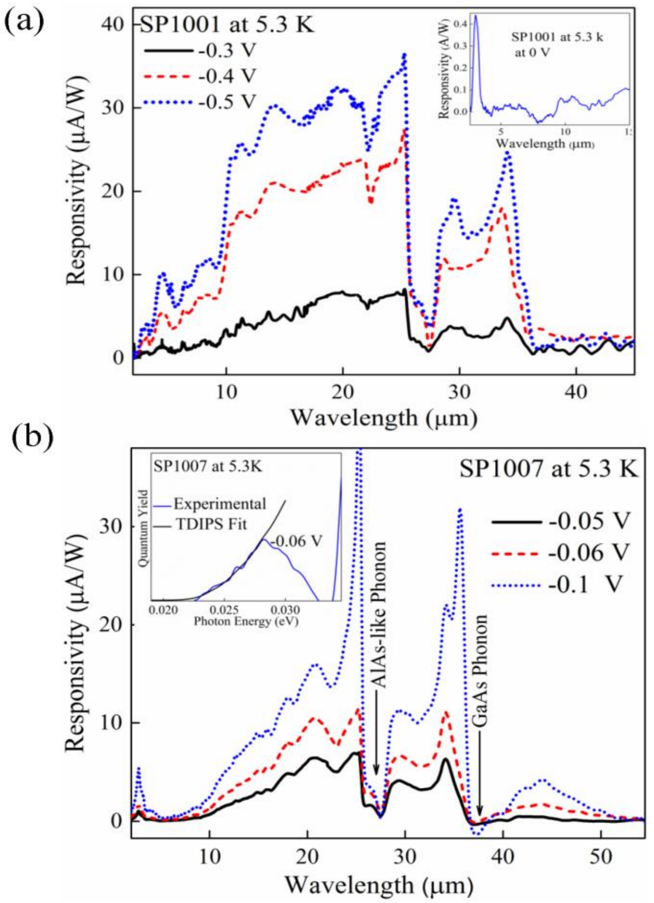

Fig. 3 (a) Experimental photoresponse of SP1001 ($\boldsymbol{\delta}E_v = 0.10$ eV) at voltages range from -0.3 to -0.5 V; an extended response up to ~36 μm is observed. However, due to a relatively high noise level, the exact threshold wavelength is not clear. Inset: extended photoresponse at 0 V, clearly showing a weak extended photoresponse starting at 0 V for SP1001 (b) Experimental photoresponse of SP1007 at a bias voltage range from -0.05 V to -0.1 V, upon application of bias extended threshold wavelength almost remains constant, however, responsivity increases with bias. Marked features are associated with GaAs and AlAs-like phonons. Inset: TDIPS fitting to determine the accurate threshold energy (Δ) of the experimental photoresponse of SP1007 at -0.06 V; the determined value of Δ is 0.0214 eV.

This article has been accepted for publication in a future issue of this journal, but has not been fully edited. Content may change prior to final publication. Citation information: DOI 10.1109/JSTQE.2017.2773622, IEEE Journal of Selected Topics in Quantum Electronics

Fig. 3(b) shows spectral photoresponse of SP1007 at different bias voltage range. By TDIPS fitting (as shown in Inset of Fig. 3(b)), an extended threshold wavelength up to ~58 μm (-0.06V) is detected. It is observed from fig. 3(a) and (b), upon application of bias, responsivity increases whereas extended threshold wavelength remains fairly constant for the spectral response of SP1001 and SP1007 at 5.3 K.

As can be seen from the schematic diagrams in figs. 2 (b) and (c)), SP1001 and SP1007 have similar device structures except the graded injector barrier in SP1007. Due to the graded barrier at the injector, the number of hot holes moving from the injector to the absorber is higher in SP1007. Thus, a longer extended threshold wavelength is observed in SP1007 due to the features seen around 40-50 µm as compare to SP1001. The sharp dip between 38-39 µm is due to the phonon absorption observed in GaAs substrates. In addition, a very strong response in the 10-25 µm range is observed in SP1001, however a physics explanation for these observations is not very much clear. Recently, an extended photoresponse of greater than 60 µm has been reported for a device structure similar to SP1007, except $\delta E_v = 0.19$ eV [15, 16].

The GaAs substrates has multiple phonon absorption lines in the region of interest that results in the valleys observed in the responsivity spectra. The marked features observed in the responsivity spectra (fig.3 (b)) are associated with GaAs and AlAs-like phonons which is already discussed elsewhere[14]. It is noted that the experimental photoresponse also exhibits two shallow valley at 22.5 μm and 32.5 μm which corresponds well with the two phonon absorption observed in GaAs substrates[26, 27].

V. SIMULATION OF EXPERIMENTAL PHOTORESPONSE

To simulate the extended threshold wavelength experimental photoresponse using an escape-cone model with a hot-hole distribution, a precise wavelength threshold in the spectral photoresponse is needed. In SP1001 ($\delta E_v = 0.10$ eV), an extended photoresponse up to ~36 μm is clearly observable (fig. 3(a)). However, the precise threshold wavelength is not clear. For SP1007, a much clearer wavelength threshold is detected, and hence we discuss simulations only of the experimental photoresponse of SP1007 in this section. A threshold energy of $\Delta = 0.0214$ eV at -0.06V, as determined by TDIPS fitting (in Inset of fig. 3(b)), is used as one of the fitting parameters in the simulation, determining the long-wavelength end of the theoretical photoresponse. By using the Δ from TDIPS fitting and value of valence band edge [25], the E_{quasiF} (i.e. valence band edge - Δ) close to 0.30 eV is determined. This is an empirical value which is used to calculate the escape probability of hot holes across the quasi-Fermi level, for the hole density in the absorber is equal to or less than that of the doping level in the absorber.

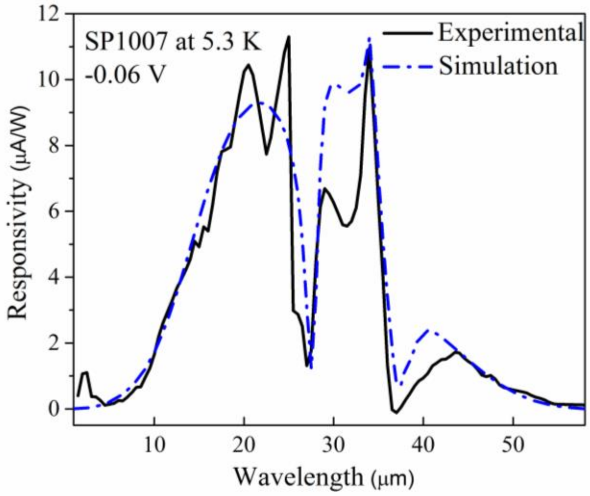

Fig.4 Comparison of Escape cone model simulated photoresponse (blue dashed line) to experimental photoresponse (solid black line) of SP1007 at a bias voltage of -0.06V at hot-hole quasi-Fermi distribution ~ 0.30 eV, with $L_h \sim 300$ nm and $L_P \sim 480$ nm. The escape of holes from quasi-Fermi distribution ~ 0.30 eV by absorption of long wavelength photon gives extended threshold wavelength photoresponse.

To simulate spectral photoresponse, the total quantum efficiency is calculated by escape-cone model[22]. For a given value of E_{quasiF}, L_h and L_p values are optimized to get significant fitting to experimental photoresponse. Fig. 4 compare experimental photoresponse (black solid line) of SP1007 (-0.06 V) to the escape cone model simulated photoresponse (blue dash line). As simulated photoresponse is clearly matched with experimental photoresponse. This simulated photoresponse when corrected for the multi phonon absorptions corresponds to 22.5 μm and 32.5 μm by using Gaussian absorption features, should further improve the fitting to be an exact match as shown previously [26].The $L_h \sim 300$ nm and $L_p \sim 480$ nm are scattering length value, where the value of $L_p > L_h$ indicates hole-phonon scattering is dominant at the quasi-Fermi distribution. Based on literature [9, 12], an average relaxation time of the order femtoseconds is estimated. The simulated results can be interpreted based on hot-cold hole dynamics in p-GaAs absorber that when hot holes interact with cold holes and finally reached quasi-Fermi distribution close to ~ 0. 30 eV, the escape of hot holes from that E_{quasiF} by absorption of long wavelength photon gives extended threshold photoresponse.

VI. CONCLUSION

We have proposed a mechanism to explain the extended threshold wavelength photoresponse in non-symmetrical p-GaAs/AlGaAs heterostructure photodetectors based on hot carrier effects. Based on the mechanism, we have simulated the extended threshold wavelength photoresponse of a non-symmetrical graded barrier heterostructures (SP1007) using a quasi-Fermi distribution of hot holes with $T_H >> T_L = 5.3$ K. The as simulated photoresponse agreed well with the experimental photoresponse for $E_{quasiF} \sim 0.30$ eV, $L_h \sim 300$ nm and $L_P \sim 480$ nm which also justifying the model used.

ACKNOWLEDGMENT

The authors are thankful to Prof. Steven Manson and Prof. V. Apalkov for their valuable suggestions and Dr. Sanjib Kabi for his involvement at the initial stage of this work.

REFERENCES

[1] N. M. Gabor, J. C. W. Song, Q. Ma, N. L. Nair, T. Taychatanapat, K. Watanabe, *et al.*, "Hot Carrier–

Assisted Intrinsic Photoresponse in Graphene," *Science,* vol. 334, pp. 648-652, 2011.

[2] Z. Sun, Z. Liu, J. Li, G.-a. Tai, S.-P. Lau, and F. Yan, "Infrared Photodetectors Based on CVD-Grown Graphene and PbS Quantum Dots with Ultrahigh Responsivity," *Advanced Materials,* vol. 24, pp. 5878-5883, 2012.

[3] W. Wang, A. Klots, D. Prasai, Y. Yang, K. I. Bolotin, and J. Valentine, "Hot Electron-Based Near-Infrared Photodetection Using Bilayer MoS2," *Nano Letters,* vol. 15, pp. 7440-7444, 2015.

[4] J. R. Hayes, A. F. J. Levi, and W. Wiegmann, "Hot-Electron Spectroscopy of GaAs," *Physical Review Letters,* vol. 54, pp. 1570-1572,1985.

[5] J. Shah, "Hot carriers in quasi-2-D polar semiconductors," *IEEE Journal of Quantum Electronics,* vol. 22, pp. 1728-1743, 1986.

[6] J. Shah, "Hot electrons and phonons under high intensity photoexcitation of semiconductors," *Solid-State Electronics,* vol. 21, pp. 43-50,1978.

[7] S. Katayama, "Theory of energy relaxation of 2D hot carriers in GaAs quantum wells," *Surface Science Letters,* vol. 170, p. A249,1986.

[8] J. Shah, A. Pinczuk, A. C. Gossard, and W. Wiegmann, "Energy-Loss Rates for Hot Electrons and Holes in GaAs Quantum Wells," *Physical Review Letters,* vol. 54, pp. 2045-2048,1985.

[9] D. J. Erskine, A. J. Taylor, and C. L. Tang, "Femtosecond studies of intraband relaxation in GaAs, AlGaAs, and GaAs/AlGaAs multiple quantum well structures," *Applied Physics Letters,* vol. 45, pp. 54-56, 1984.

[10] J. Shah, A. Pinczuk, H. L. Störmer, A. C. Gossard, and W. Wiegmann, "Electric field induced heating of high mobility electrons in modulation-doped GaAs-AlGaAs heterostructures," *Applied Physics Letters,* vol. 42, pp. 55-57, 1983.

[11] J. Shah, "Investigation of hot carrier relaxation with picosecond laser pulses," *J. Phys. Colloques,* vol. 42, pp. C7-445-C7-462, 1981.

[12] R. W. Schoenlein, W. Z. Lin, E. P. Ippen, and J. G. Fujimoto, "Femtosecond hot-carrier energy relaxation in GaAs," *Applied Physics Letters,* vol. 51, pp. 1442-1444, 1987.

[13] C. V. Shank, R. L. Fork, R. Yen, J. Shah, B. I. Greene, A. C. Gossard, *et al.*, "Picosecond dynamics of hot carrier relaxation in highly excited multi-quantum well structures," *Solid State Communications,* vol. 47, pp. 981-983, 1983.

[14] Y.-F. Lao, A. G. U. Perera, L. H. Li, S. P. Khanna, E. H. Linfield, and H. C. Liu, "Tunable hot-carrier photodetection beyond the bandgap spectral limit," *Nat Photon,* vol. 8, pp. 412-418, 2014.

[15] D. Chauhan, A. G. U. Perera, L. Li, L. Chen, S. P. Khanna, and E. H. Linfield, "Extended wavelength infrared photodetectors," *Optical Engineering,* vol. 56, pp. 091605-091605, 2017.

[16] D. Chauhan, A. G. U. Perera, L. H. Li, L. Chen, and E. H. Linfield, "Dark current and photoresponse characteristics of extended wavelength infrared photodetectors," *Journal of Applied Physics,* vol. 122, p. 024501, 2017.

[17] S. G. Matsik, P. V. V. Jayaweera, A. G. U. Perera, K. K. Choi, and P. Wijewarnasuriya, "Device modeling for split-off band detectors," *Journal of Applied Physics,* vol. 106, p. 064503, 2009.

[18] A. G. U. Perera, H. X. Yuan, and M. H. Francombe, "Homojunction internal photoemission far-infrared detectors: Photoresponse performance analysis," *Journal of Applied Physics,* vol. 77, pp. 915-924, 1995.

[19] D. G. Esaev, M. B. M. Rinzan, S. G. Matsik, and A. G. U. Perera, "Design and optimization of GaAs⁄AlGaAs heterojunction infrared detectors," *Journal of Applied Physics,* vol. 96, pp. 4588-4597, 2004.

[20] Y.-F. Lao, A. G. U. Perera, L. H. Li, S. P. Khanna, E. H. Linfield, and H. C. Liu, "Direct observation of spin-orbit splitting and phonon-assisted optical transitions in the valence band by internal photoemission spectroscopy," *Physical Review B,* vol. 88, p. 201302, 2013.

[21] R. G. Ulbrich, "Low density photoexcitation phenomena in semiconductors: Aspects of theory and experiment," *Solid-State Electronics,* vol. 21, pp. 51-59, 1978.

[22] M. B. Rinzan, S. Matsik, and A. G. U. Perera, "Quantum mechanical effects in internal photoemission THz detectors," *Infrared Physics & Technology,* vol. 50, pp. 199-205, 2007.

[23] P. Pitigala, Y. Lao, A. Perera, L. Li, E. Linfield, and H. Liu, "Performance improvements of a split-off band infra-red detector using a graded barrier," *Journal of Applied Physics,* vol. 115, p. 063105, 2014.

[24] Y.-F. Lao, A. U. Perera, Y. Zhang, and T. Wang, "Band-offset non-commutativity of GaAs/AlGaAs interfaces probed by internal photoemission spectroscopy," *Applied Physics Letters,* vol. 105, p. 171603, 2014.

[25] Y.-F. Lao and A. G. U. Perera, "Temperature-dependent internal photoemission probe for band parameters," *Physical Review B,* vol. 86, p. 195315, 2012.

[26] A. G. U. Perera, S. G. Matsik, H. C. Liu, M. Gao, M. Buchanan, W. J. Schaff, *et al.*, "GaAs/InGaAs quantum well infrared photodetector with a cutoff wavelength at 35 μm," *Applied Physics Letters,* vol. 77, pp. 741-743, 2000.

[27] J. S. Blakemore, "Semiconducting and other major properties of gallium arsenide," *Journal of Applied Physics,* vol. 53, pp. R123-R181,1982.

Divya Somvanshi received the B.Sc., M.Sc., and Ph.D. degrees from the Government Degree College, Hardoi, India, in 2005; D.A.V. College, Kanpur, India, in 2007; and the Indian Institute of Technology (BHU), Varanasi, India, in 2015, respectively. She was a Research Associate with the Department of Electrical and Communication Engineering, Indian Institute of Science, Bangalore from June 2015 to March 2016. She is currently working as a Postdoctoral Researcher at Department of Physics and Astronomy, Georgia State University, Atlanta USA. Her current research interests focus on the analysis and characterization of novel hot carrier photodetectors based on GaAs/AlGaAs heterostructures.

Dilip Chauhan received the B. Sc. and M. Sc. degrees in Physics from Tribhuvan University, Kathmandu, Nepal in 2007, and 2009 respectively. He is currently a Ph.D. candidate at the Department of Physics and Astronomy at Georgia State University (GSU), Atlanta. His research interests include design and development of semiconductor material-based infrared photodetectors for mid-infrared detection at high operating temperatures, and hot-carrier enabled extended wavelength infrared photodetectors for mid-infrared to terahertz range. He has also been a Brain & Behavior Fellow at the Neuroscience Institute, GSU since 2013.

Yanfeng Lao received the B.S. and M.S. degrees in physics from Zhejiang University, Hangzhou, China, in 1999 and 2002, respectively, and the Ph.D. degree in microelectronics and solid-state electronics from the Shanghai Institute of Microsystem and Information Technology, Shanghai, China, in 2007. He was a Postdoctoral Researcher and Research Scientist with the Department of Physics and Astronomy, Georgia State University (GSU), Atlanta, working on material characterizations and infrared photodetectors based on split-off and novel hot-carrier concepts. He is currently working as a laser device engineer at Archcom Technology Inc., South Plainfield, NJ. His work involves the molecular beam epitaxial growth of III–V semiconductor compounds, semiconductor lasers, photodetectors and related modeling and simulations.

A. G. Unil Perera received the B.S. degree in physics (with first class honors) from the University of Colombo, Colombo, Sri Lanka, and the M.S. and Ph.D. degrees from the University of Pittsburgh. He is currently a Regents' Professor at the Department of Physics and Astronomy, Georgia State University, Atlanta. He is a Fellow of the IEEE, SPIE and APS. He has served on the National Science Foundation, Department of Energy, and National Aeronautics and Space Administration proposal review panels and also as a reviewer for numerous research proposals and papers. His present research (supported by NSF and DOD) focus is on developing tunable and bias selectable detectors responding from UV to FIR. He has 8 US patents, 4 edited books, 11 invited book chapters and over 175 publications. He is also a member of the editorial board for the IEEE Journal of Electron Device Society.

Lianhe Li received the Ph.D. degree in microelectronics and solid-state electronics from the Institute of Semiconductors, Chinese Academy of Sciences, China, in 2001. From 2001 to 2003, he was with the Laboratoire de Photonique et des Nanostructures, Centre National de la Recherche Scientifique, France. Then, he joined École polytechnique fédérale de Lausanne, Switzerland, as a Scientific Collaborator, working on InAs quantum dots for lasers and super luminescent LEDs and single quantum dot devices. Since 2008, he has been with the School of Electronic and Electrical Engineering, University of Leeds, U.K. His current research interests focus on the molecular beam epitaxy growth and characterization of semiconductor materials and devices with a particular emphasis on mid-infrared and terahertz-frequency generation and detection.

Suraj Parkash Khanna received the Ph.D. degree in Electronic and Electrical Engineering (2004-2008) from the University of Leeds, Leeds, UK. He continued his research at the University of Leeds as a Post-Doctoral Research Associate until 2011. He was engaged in research on molecular beam epitaxial growth, semiconductor device fabrication, quantum cascade lasers and terahertz frequency optical systems. Thereafter he spent a year at the Northwestern University, Evanston, USA as a Research Fellow working on MOCVD growth of dilute magnetic semiconductors. In 2012, he moved to the CSIR-National Physical Laboratory, New Delhi, India, where he is currently the Principal Scientist in the division 2D Physics and Quantum Resistance Metrology. His current research interests include hybrid heterostructure devices based on the integration of bulk semiconductors with 2D layered (van der Waals) materials for optoelectronic applications.

Edmund Harold Linfield received the B.A.(Hons.) degree in Physics and the Ph.D. degree from the University of Cambridge, Cambridge, U.K., in 1986 and 1991, respectively. He continued his research at the Cavendish Laboratory, University of Cambridge, becoming an Assistant Director of Research and a Fellow of Gonville and Caius College, Cambridge, U.K. in 1997. In 2004, he joined the University of Leeds to take up the Chair of Terahertz Electronics where he is currently also the Director of Research and Innovation in the School of Electronic and Electrical Engineering. His research interests include semiconductor growth and device fabrication, terahertz-frequency optics and electronics, and nanotechnology. Professor Linfield shared the Faraday Medal and Prize from the Institute of Physics in 2014, and received a Wolfson Research Merit Award from the Royal Society in 2015.